Physics-Informed Learning of Joint Dynamics in Articulated Robots

Rupam Singh, Smith Khare, Varaha Satya Bharath Kurukuru

Abstract— **Modeling the dynamics of articulated robotic hands presents significant challenges due to high degrees of freedom, nonlinear interactions, and sensitivity to external forces. Traditional rigid-body models often oversimplify system behavior, while standard neural networks (NNs) may introduce energy drift and instability in long-term predictions. This paper examines the effectiveness of Physics-Informed Neural Networks (PINNs) in capturing the dynamic behavior of articulated hand joints while preserving physical consistency. By incorporating energy conservation principles and accounting for coupled joint interactions, PINNs provide improved stability compared to conventional data-driven models. Through comparative simulations, the advantages and limitations of PINNs in modeling are analyzed, demonstrating their ability to enhance dynamic accuracy and maintain energy consistency. Results demonstrate that PINNs reduce root mean square error (RMSE) by an average of 20% compared to baseline NNs, confirming their improved predictive accuracy and robustness in handling dynamic perturbations.**

I. INTRODUCTION

Modeling and controlling the dynamics of articulated robotic hands is challenging due to the system's numerous joints and degrees of freedom (DOF). Traditional rigid-body dynamic models often fail to capture the nonlinear interactions between joints, tendons, and external forces, leading to inaccuracies, especially over extended periods or in unstructured environments [1]. These models tend to oversimplify system behavior by neglecting key physical properties such as energy conservation and damping effects, limiting their ability to simulate realistic motion [2].

Various approaches have been proposed to model robotic system dynamics, each with distinct advantages and limitations. Traditional physics-based models, including Lagrangian and Euler-Lagrange formulations, provide explicit mathematical representations but struggle to accurately capture joint elasticity, damping effects, and nonlinear inter-joint interactions in high-DOF robotic hands [3], [4]. Data-driven methods, particularly neural networks (NNs), have gained attention due to their ability to capture complex motion patterns without explicit mathematical models [7], [8]. However, standard NNs lack physical consistency, often leading to energy drift and instability in long-term predictions. Deep reinforcement learning (DRL) models have also been applied to dexterous robotic manipulation [9], [10], but they focus on policy learning rather than direct dynamic modeling and frequently fail to conserve fundamental physical quantities like energy and momentum, impacting stability [11].

Physics-Informed Neural Networks (PINNs) address these limitations by incorporating physical constraints, such as energy conservation, into the learning process, ensuring more accurate long-term predictions [12], [13]. Unlike standard NNs that rely purely on data, PINNs enforce physical priors, improving stability and interpretability in dynamic modeling. Compared to DRL-based methods, PINNs focus on system dynamics rather than control policies, making them particularly effective for applications requiring long-term predictive accuracy.

Beyond theoretical advancements, accurate dynamic modeling of articulated robotic hands is essential in real-world applications. In robotic-assisted surgery, precise joint movement prediction ensures stable tool manipulation and minimizes unintended forces on delicate tissues. In prosthetics, long-term joint dynamics modeling enables smoother, more natural movement, enhancing functionality. Similarly, industrial robotic manipulators rely on stable finger dynamics for high-precision assembly tasks, particularly in automated manufacturing. Ensuring energy consistency and stability in articulated robotic hands is critical for these applications, reinforcing the need for physically informed predictive models. PINNs, especially those applied to robotic systems, overcome the limitations of baseline NNs by integrating Hamiltonian mechanics, improving both physical interpretability and predictive accuracy [14], [15], [16]. Recent studies emphasize the importance of incorporating energy conservation constraints to enhance model robustness and stability, particularly in systems where small errors in energy estimation accumulate over time, affecting performance [17]. Such models have demonstrated improved reliability in control tasks, making them suitable for high-precision applications [18], [19].

This paper adapts Hamiltonian mechanics to enhance NN-based models for predicting articulated robotic hand dynamics. By integrating physical laws into the learning process, the proposed hybrid approach addresses the limitations of standard NNs in dynamic modeling. PINNs ensure physically consistent predictions, leading to more accurate and stable long-term simulations. The major contributions of this research are:

- A detailed mathematical formulation for modeling coupled joint dynamics in articulated robotic hands using spring-mass-damper systems, capturing inter-joint inter-

[1]Rupam Singh is with Faculty of Engineering, Maersk Mc-Kinney Moller Institute, SDU Robotics, Syddansk Universitet, Campusvej 55, 5230 Odense M, Denmark. [2]Smith K. Khare is with Faculty of Engineering, Maersk Mc-Kinney Moller Institute, SDU Applied AI and Data Science, Syddansk Universitet, Campusvej 55, 5230 Odense M, Denmark. [3]Varaha Satya Bharath Kurukuru is with Research Division Power ELectronics, Silicon Austria Labs GmbH, 9524 Villach, Austria. [1]rupsi@mmmi.sdu.dk, [2]smkh@mmmi.sdu.dk, [3]varaha.kurukuru@silicon-austria.com

actions.

- The development of a Hamiltonian-based PINN framework that enforces energy conservation and physical laws to improve long-term predictive accuracy in dynamic systems.
- Extensive simulations demonstrating the effectiveness of the PINN model in comparison to baseline NNs, highlighting superior performance in maintaining energy stability and accurate long-term predictions.

Further sections of this paper are organized as follows: Section 2 introduces the mathematical framework for modeling articulated hand joints as a spring-mass-damper system. Section 3 defines the application of NNs for dynamic prediction, highlighting their limitations. It also presents the integration of Hamiltonian mechanics into NNs, describing the PINN framework. Section 4 provides simulation results comparing baseline NNs and PINNs, while Section 5 concludes with a discussion of the findings.

II. Modeling an Articulated Hand with a Spring-Mass-Damper System

A. Single Joint Dynamics

The motion of a single joint in an articulated hand can be modeled as a rotational spring-mass-damper system, where the joint rotates about a fixed axis [15]. The rotational analog of Newton's second law describes the joint's dynamics. For angular position $\mathbf{q}(t)$, the equation of motion is:

$$\mathbf{J}\frac{d^2\mathbf{q}(t)}{dt^2}+\mathbf{B}\frac{d\mathbf{q}(t)}{dt}+\mathbf{K}\mathbf{q}(t)=\tau_{\text{ext}}(t), \tag{1}$$

where $\mathbf{J}$ is rotational inertia, $\mathbf{B}$ is the damping coefficient, and $\mathbf{K}$ represents stiffness. The term $\tau_{\text{ext}}(t)$ denotes the external torque applied to the joint.

This spring-mass-damper analogy effectively models robotic joint dynamics, where tendon elasticity is represented as springs, and damping accounts for frictional resistance. External torques include actuator forces and environmental interactions.

B. Finger Joint Dynamics

A robotic finger consists of multiple joints in series. Fig. 1 illustrates the mechanical model, where a spring-mass system captures joint dynamics and flexure compliance [15]. The tendon routing system constrains out-of-plane motions. Each flexure joint is modeled as a spring-damper, while phalanges are treated as masses. The flexion/extension motions of the distal, proximal, and metacarpophalangeal (MCP) joints correspond to the displacements x_d, x_p, and x_{fm}, while adduction/abduction is modeled as rotation about the θ-axis. The generalized dynamics for a finger with n joints follows:

$$\mathbf{J}_i\frac{d^2\mathbf{q}_i(t)}{dt^2}+\mathbf{B}_i\frac{d\mathbf{q}_i(t)}{dt}+\mathbf{K}_i\mathbf{q}_i(t)=\tau_{\text{ext},i}(t), \tag{2}$$

for $i=1,2,...,n$, where $\mathbf{J}_i$, $\mathbf{B}_i$, and $\mathbf{K}_i$ are the rotational inertia, damping, and stiffness coefficients of joint i. The external torque $\tau_{\text{ext},i}(t)$ varies based on applied forces.

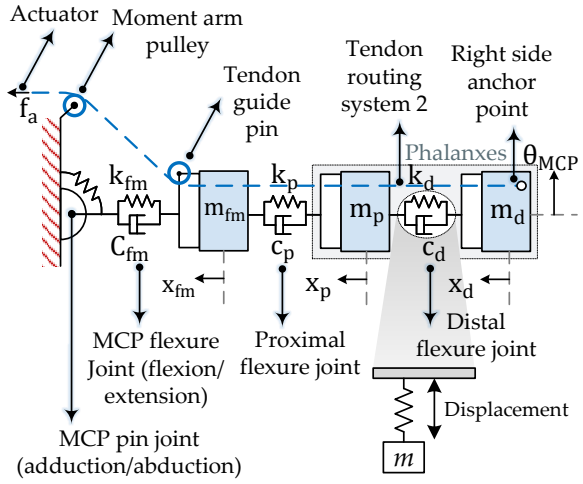

Fig. 1. Mechanical model of a robotic finger with spring-damper flexure joints and tendon routing systems, illustrating flexion/extension and adduction/abduction motions.

Finger dynamics are governed by coupled differential equations, where each joint's motion affects adjacent joints through tendons, linkages, or compliant structures [16]. Interaction forces introduce coupling terms dependent on joint positions and velocities. The generalized dynamics, incorporating inter-joint torques, is:

$$\mathbf{J}_i\frac{d^2\mathbf{q}_i(t)}{dt^2}+\mathbf{B}_i\frac{d\mathbf{q}_i(t)}{dt}+\mathbf{K}_i\mathbf{q}_i(t)=\tau_{\text{ext},i}(t)+\sum_{j\in\mathcal{N}_i}\tau_{\text{int},ij}(t), \tag{3}$$

where $\mathcal{N}_i$ denotes neighboring joints coupled to i, and $\tau_{\text{int},ij}(t)$ represents interaction torques, modeled as:

$$\tau_{\text{int},ij}(t)=k_{ij}(\mathbf{q}_j(t)-\mathbf{q}_i(t))+b_{ij}\left(\frac{d\mathbf{q}_j(t)}{dt}-\frac{d\mathbf{q}_i(t)}{dt}\right), \tag{4}$$

where k_{ij} and b_{ij} are the coupling stiffness and damping coefficients.

C. Dynamics of an Articulated Hand

An articulated hand consists of multiple fingers, each with several joints. The system is modeled as interconnected spring-mass-damper systems, where each joint follows the same governing principles. Let m represent the number of fingers, each with n_j joints. The complete hand dynamics are expressed as:

$$\sum_{j=1}^{m}\sum_{i=1}^{n_j}\left(\mathbf{J}_{j,i}\frac{d^2\mathbf{q}_{j,i}(t)}{dt^2}+\mathbf{B}_{j,i}\frac{d\mathbf{q}_{j,i}(t)}{dt}+\mathbf{K}_{j,i}\mathbf{q}_{j,i}(t)\right)=\tau_{\text{ext},H}(t), \tag{5}$$

where $\mathbf{J}_{j,i}$, $\mathbf{B}_{j,i}$, and $\mathbf{K}_{j,i}$ are the inertia, damping, and stiffness matrices of the i-th joint of finger j, $\mathbf{q}_{j,i}(t)$ is its angular position, and $\tau_{\text{ext},H}(t)$ represents external torques on the hand.

The coupled nature of the system implies that joint motion is influenced by neighboring joints and interaction forces

between fingers. The increasing complexity with additional fingers and joints makes the spring-mass-damper model an efficient framework for analyzing robotic hand dynamics.

III. Learning-Based Dynamics Prediction for Robotic Systems

The articulated hand model described earlier captures joint dynamics using a spring-mass-damper system, incorporating external forces, stiffness, and damping. While structured, predicting future states of such a nonlinear system remains challenging. Standard NNs offer a data-driven approach but often lack physical consistency, leading to instability over long-term predictions. PINNs address this by integrating physical constraints into the learning process. This section evaluates both approaches for modeling articulated robotic systems.

A. Neural Network-Based Dynamics Modeling

NNs learn system dynamics from observed motion data by analyzing joint positions, velocities, and applied torques. The system is formulated as a mapping function where current joint states predict future states. Mathematically, a joint's state at time t is characterized by angular position $q(t)$ and angular momentum $p(t)$, and the NN approximates:

$$f_{\text{NN}} : (q(t), p(t)) \to (q(t+1), p(t+1)). \tag{6}$$

Training minimizes a loss function, typically the mean squared error (MSE) between predicted and actual states:

$$\text{Loss} = \frac{1}{N}\sum_{i=1}^{N}\left[\left(q_i^{\text{pred}} - q_i^{\text{true}}\right)^2 + \left(p_i^{\text{pred}} - p_i^{\text{true}}\right)^2\right]. \tag{7}$$

Despite capturing short-term behavior, standard NNs lack explicit physical constraints, causing energy drift over time. In robotic systems such as an articulated hand, where energy should be conserved unless external forces act, this issue is particularly problematic. The total mechanical energy, consisting of kinetic energy T and potential energy V, is expected to remain constant in the absence of external inputs:

$$H(q,p) = T(q,p) + V(q) = \text{constant}. \tag{8}$$

Conventional NNs fail to model interactions between angular position, momentum, and energy conservation. Kinetic energy in rotational systems depends on angular momentum and inertia, while potential energy is governed by joint stiffness. Without explicit constraints, NN predictions may become physically inconsistent over extended time horizons.

NNs predict future states based on joint positions, velocities, and torques without enforcing physical constraints. External torques τ_{ext} influence dynamics but are often treated as forcing terms rather than intrinsic variables. Since their evolution is typically unknown, effects are captured indirectly through observed trajectories during training. While factors such as angular position $q(t)$, momentum $p(t)$, stiffness K, and damping B influence predictions, the absence of physical priors leads to inaccuracies. PINNs overcome this limitation by incorporating governing equations, such as the Hamiltonian formulation, to enforce energy conservation. By minimizing a loss function that includes Hamiltonian derivatives, PINNs improve long-term stability while preserving physical accuracy, as illustrated in Fig. 2.

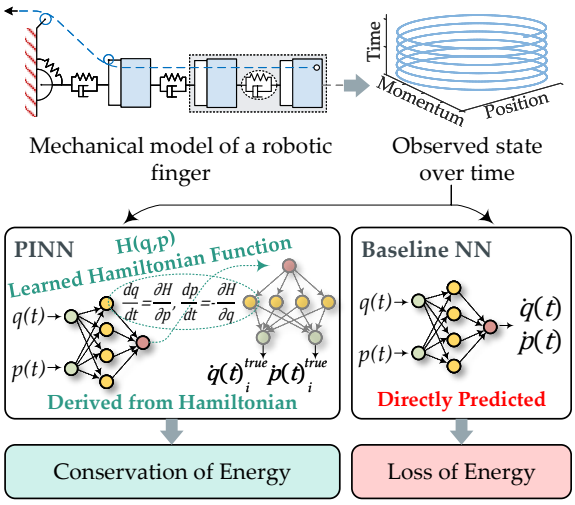

Fig. 2. Comparison of baseline NN and PINN for modeling articulated robotic finger dynamics.

B. Physics-Informed Neural Networks for Energy-Conserving Dynamics

PINNs introduce physical constraints directly into the learning process by modeling system dynamics using the Hamiltonian function $H(q,p)$, which represents total system energy [17]. Instead of directly predicting future states, the PINN learns $H(q,p)$ and derives system evolution through Hamilton's equations [18]:

$$\frac{dq}{dt} = \frac{\partial H}{\partial p}, \quad \frac{dp}{dt} = -\frac{\partial H}{\partial q}. \tag{9}$$

where $H(q,p)$ is the sum of kinetic and potential energy:

$$H(q,p) = \frac{p^2}{2J} + \frac{1}{2}kq^2. \tag{10}$$

This ensures energy conservation by constraining the evolution of generalized coordinates q and momenta p. The first term represents kinetic energy, governed by system inertia J, while the second accounts for potential energy, defined by stiffness k. The Hamiltonian framework enforces a natural energy exchange, preventing artificial energy dissipation or accumulation. Rather than mapping joint states to time derivatives, PINNs learn the energy function and use its gradients to derive system evolution. This guarantees that predicted trajectories adhere to system physics, making PINNs particularly suited for long-term stability in articulated joint dynamics. While the Hamiltonian formulation assumes ideal energy-conserving systems, real-world dissipative effects such as friction can be approximated in the PINN framework by introducing additional damping-like loss terms or treating them as external forces, allowing the network to

learn dissipative behaviors during training.

In cases where J and k are uncertain, PINNs incorporate trainable parameters to estimate these values during learning, reducing reliance on exact prior knowledge. This adaptation maintains physical consistency even in systems with unknown variations. Training involves minimizing the discrepancy between the learned and true time derivatives:

$$\text{Loss} = \frac{1}{N}\sum_{i=1}^{N}\left[\left(\frac{\partial H}{\partial p_i} - \dot{q}_i^{\text{true}}\right)^2 + \left(\frac{\partial H}{\partial q_i} + \dot{p}_i^{\text{true}}\right)^2\right]. \quad (11)$$

The first term penalizes velocity prediction errors, ensuring consistency between $\dot{q}_i$ and $\frac{\partial H}{\partial p_i}$, while the second enforces accurate acceleration predictions by constraining $\dot{p}_i$ to follow $-\frac{\partial H}{\partial q_i}$. Unlike standard loss functions relying solely on trajectory matching, this formulation leverages the system's inherent energy properties for learning.

By minimizing this loss, PINNs refine their approximation of $H(q,p)$ while preserving energy balance between kinetic and potential components. In the absence of external forces, total energy remains constant, ensuring physically plausible motion even over extended simulations. This formulation is crucial in articulated robotic hands, where joint motion is influenced by coupled interactions, and long-term stability is essential for accurate dynamic modeling.

IV. Simulation and Results

This section presents the simulation process for both the baseline NN and the PINN. Both models were trained on a dataset of 750 samples, each containing 4 features per row, the first two columns represent input state variables (e.g., position q, momentum p), and the last two represent their corresponding time derivatives (e.g., $\dot{q}$, $\dot{p}$). This structure allows the models to learn the underlying system dynamics. The models are trained, evaluated, and compared based on their ability to replicate the dynamics of an underdamped spring-mass-damper system, serving as a simplified representation of articulated joint dynamics. The selection of parameters **J**, **B**, and **K**, as discussed in Section II, was based on prior studies on robotic systems [20]. Stiffness values between 0.5 Nm/rad and 2.0 Nm/rad were chosen to balance joint flexibility and resistance, with $K = 1.294$ Nm/rad used in simulations. The damping coefficient was set within 0.05 Nms/rad to 0.5 Nms/rad to regulate oscillations while avoiding excessive restriction, with $B = 0.847$ Nms/rad selected. Rotational inertia values ranged from 0.0005 kg·m² to 0.02 kg·m² to ensure realistic responses without excessive computational cost. The final value of $J = 0.523$ kg·m² provides a compromise between responsiveness and stability.

A. Baseline Neural Network Simulation

The baseline NN predicts future joint states $q(t)$ and $p(t)$ from the current state $[q(t), p(t)]$, outputting $[q(t+1), p(t+1)]$. The architecture consists of fully connected layers with *tanh* activation. Training minimizes the MSE between predicted and true states using the Adam optimizer. Key hyperparameters include 300 epochs, a mini-batch size of 750, an initial learning rate of 0.001, and a decay rate of $1e^{-4}$. While the model minimizes short-term errors, iterative updates introduce drift due to the absence of explicit physical constraints, affecting long-term accuracy. Fig. 3(a) shows model convergence, with loss stabilizing after 50 iterations at 0.03749 by epoch 300. Fig. 3(b) presents the phase space, where circular trajectories suggest stable oscillations, though minor deviations indicate incomplete energy conservation. Fig. 3(c) illustrates position and momentum trajectories, revealing periodic spiral-like paths. Fig. 4 shows kinetic and potential energy evolution, where periodic exchanges are observed, but an overall energy decay confirms that the baseline NN fails to maintain energy consistency, leading to physically unrealistic long-term predictions.

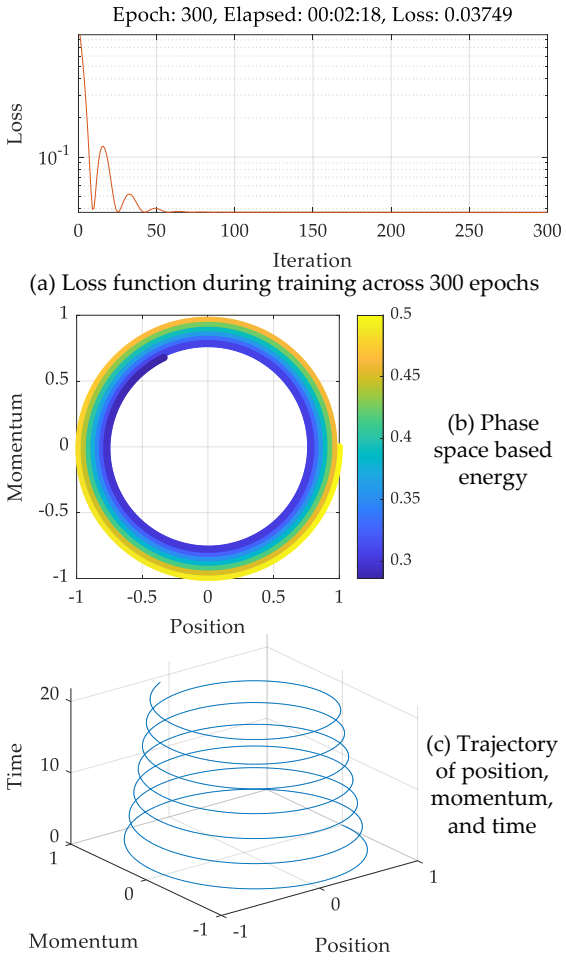

Fig. 3. Training Dynamics and Model Performance for NN

B. PINN Simulation

The PINN models system dynamics through the Hamiltonian function $H(q,p)$, representing total energy. Inputs include initial states $q(0), p(0)$ and trajectory data containing $dq/dt, dp/dt$. Instead of directly predicting future states, the PINN learns an approximate Hamiltonian, from which time derivatives are computed. Similar to the baseline NN, training uses the Adam optimizer, with hyperparameters con-

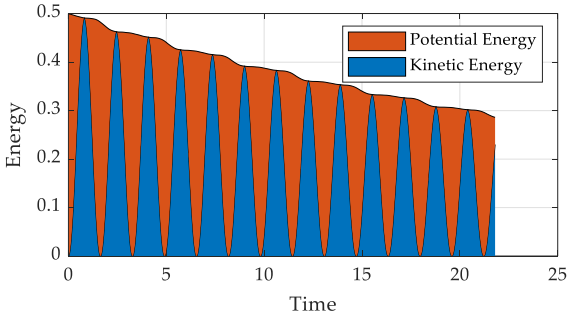

Fig. 4. Energy Dynamics and Conservation for the Baseline NN

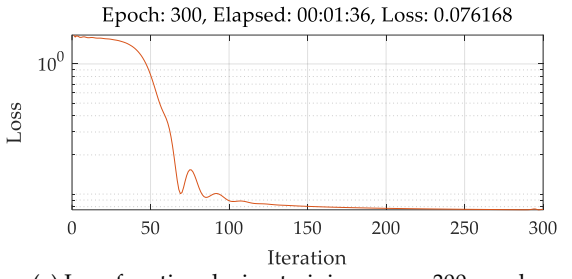

(a) Loss function during training across 300 epochs

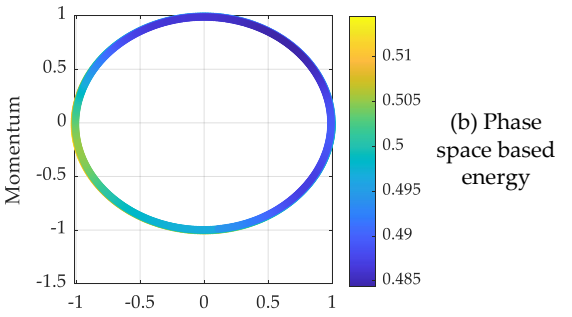

(b) Phase space based energy

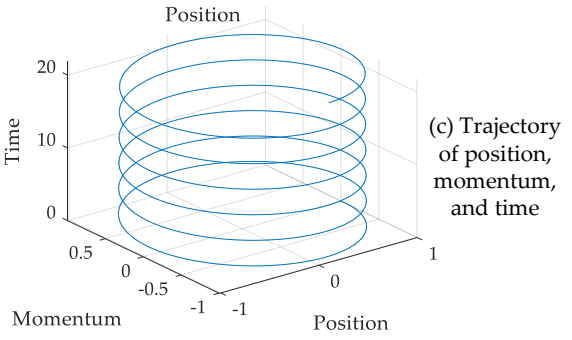

(c) Trajectory of position, momentum, and time

Fig. 5. Training Dynamics for PINN

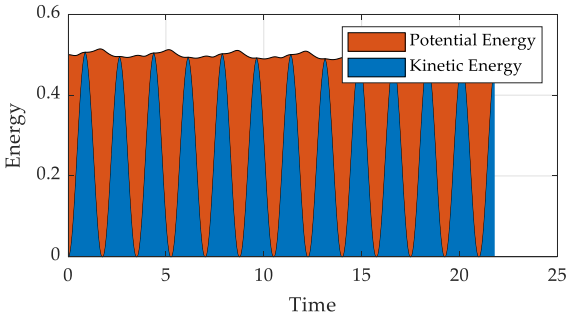

Fig. 6. Energy Dynamics and Conservation for the PINN

trolling convergence. By enforcing energy conservation principles, the PINN improves long-term stability and captures joint interactions more effectively. Training and simulation results are shown in Fig. 5 and 6.

Fig. 5(a) shows loss convergence around 100 iterations, reaching 0.01 by epoch 300. Fig. 5(b) depicts the phase space with energy color coding, showing near-perfect circular trajectories, confirming energy conservation and stable dynamics. Fig. 5(c) illustrates joint motion, where periodic spirals indicate accurate long-term stability. Fig. 6 presents kinetic and potential energy evolution, where alternating peaks reflect consistent energy exchange, and total energy remains nearly constant, demonstrating the model's ability to conserve energy even in multi-joint systems.

C. Comparative Analysis of Energy Conservation and Stability

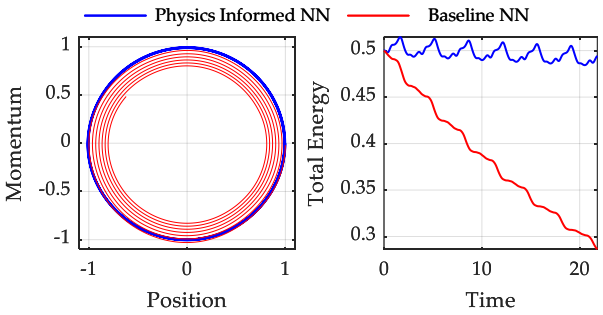

(a) Phase Space of trajectory (b) Total energy overtime

Fig. 7. Comparison of baseline NN and PINN in Energy Conservation and System Dynamics

The results in Fig. 7 highlight differences between the baseline NN and PINN. Fig. 7(a) presents phase space trajectories, where the PINN produces nearly perfect circular orbits, preserving energy, while the baseline NN shows trajectory drift, confirming its inability to maintain stability. Fig. 7(b) illustrates total energy evolution, where the PINN maintains consistency, while the baseline NN exhibits energy decay, leading to physically unrealistic predictions. These findings confirm that integrating physical constraints enhances stability, making PINNs more suitable for articulated robotic systems. Fig. 8 quantifies predictive accuracy using RMSE and MAE. The PINN achieves a median RMSE of 0.83 compared to 1.00 for the baseline NN, with a lower maximum error of 1.09. For MAE, the PINN reduces median error to 0.42, while the baseline NN reaches 0.58. For the dynamics of an underdamped spring-mass-damper system, the PINN consistently outperforms the baseline NN, achieving an average RMSE reduction of 20%. This demonstrates that the PINN maintains stable predictions, while the NN exhibits higher error accumulation, confirming its limitations in handling dynamic perturbations. This improvement translates to more accurate joint motion predictions, which is critical for real-world manipulation tasks requiring sub-millimeter precision—such as surgical tool handling or precision assembly, where typical error tolerances range from

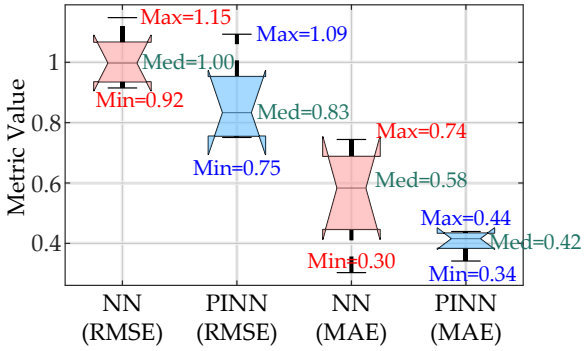

Fig. 8. Comparison of PINN and baseline NN for RMSE and MAE across multiple joints. The PINN demonstrates lower error variance and improved stability under varying conditions.

0.5 to 2.0 mm.

The results confirm that the baseline NN struggles with multi-joint interactions, where trajectory drift and energy decay compound over multiple joints. In contrast, the PINN effectively models inter-joint couplings, ensuring energy transfer between joints aligns with physical laws. This is particularly important for high-degree-of-freedom robotic systems, where inaccurate predictions can lead to unstable motion control. By enforcing energy conservation and coupling constraints, the PINN provides a robust framework for modeling articulated hand dynamics, offering improved accuracy in long-term simulations.

V. Conclusion

This research examines the effectiveness of PINNs in modeling the dynamics of articulated robotic hands while preserving physical consistency. By incorporating Hamiltonian mechanics, particularly energy conservation principles, PINNs address the limitations of baseline NNs, which exhibit energy drift and instability in long-term predictions. Comparative simulations demonstrate that PINNs outperform baseline NNs in maintaining stable system dynamics, accurately capturing joint interactions, and ensuring energy consistency. Results indicate that the PINN reduces RMSE by an average of 20%, achieving a median RMSE of 0.83 compared to 1.00 for the NN, while also reducing median MAE from 0.58 to 0.42. These improvements highlight the advantages of enforcing physical constraints in neural network models, ensuring long-term stability and predictive accuracy in robotic manipulation tasks. Future work will explore modeling complex contact dynamics, and optimizing training for real-time applications.

References

[1] Yu C and Wang P (2022) Dexterous Manipulation for Multi-Fingered Robotic Hands With Reinforcement Learning: A Review. Front. Neurorobot. 16:861825. doi: 10.3389/fnbot.2022.861825

[2] Y. Yang, X. Chen, and Y. Han, "Dadu-RBD: Robot Rigid Body Dynamics Accelerator with Multifunctional Pipelines," in 56th Annual IEEE/ACM International Symposium on Microarchitecture, Oct. 2023, pp. 297–309. doi: 10.1145/3613424.3614298.

[3] Z. Liu, O. Zhang, Y. Gao, Y. Zhao, Y. Sun and J. Liu, "Adaptive Neural Network-Based Fixed-Time Control for Trajectory Tracking of Robotic Systems," in IEEE Transactions on Circuits and Systems II: Express Briefs, vol. 70, no. 1, pp. 241-245, Jan. 2023, doi: 10.1109/TCSII.2022.3194917.

[4] A. Petrenko, A. Allshire, G. State, A. Handa, and V. Makoviychuk, "DexPBT: Scaling up Dexterous Manipulation for Hand-Arm Systems with Population Based Training." 2023. [Online]. Available: https://arxiv.org/abs/2305.12127

[5] C. Tang, B. Abbatematteo, J. Hu, R. Chandra, R. Martín-Martín, and P. Stone, "Deep Reinforcement Learning for Robotics: A Survey of Real-World Successes." 2024. [Online]. Available: https://arxiv.org/abs/2408.03539

[6] Banerjee, Chayan and Nguyen, Kien and Fookes, Clinton and Raissi, Maziar, A Survey on Physics Informed Reinforcement Learning: Review and Open Problems. Available at SSRN: https://ssrn.com/abstract=4597487 or http://dx.doi.org/10.2139/ssrn.4597487

[7] Y. Qin et al., "AnyTeleop: A General Vision-Based Dexterous Robot Arm-Hand Teleoperation System." 2024. [Online]. Available: https://arxiv.org/abs/2307.04577

[8] J. Ye, J. Wang, B. Huang, Y. Qin, and X. Wang, "Learning Continuous Grasping Function With a Dexterous Hand From Human Demonstrations," IEEE Robot. Autom. Lett., vol. 8, no. 5, pp. 2882–2889, 2023, doi: 10.1109/LRA.2023.3261745.

[9] M. Raissi, P. Perdikaris, and G. E. Karniadakis, "Physics-informed neural networks: A deep learning framework for solving forward and inverse problems involving nonlinear partial differential equations," J. Comput. Phys., vol. 378, pp. 686–707, Feb. 2019, doi: 10.1016/j.jcp.2018.10.045.

[10] Chen, Z., Liu, Y. and Sun, H. Physics-informed learning of governing equations from scarce data. Nat Commun 12, 6136 (2021). https://doi.org/10.1038/s41467-021-26434-1

[11] G. Chirco, L. Malagò, and G. Pistone, "Lagrangian and Hamiltonian dynamics for probabilities on the statistical bundle," Int. J. Geom. Methods Mod. Phys., vol. 19, no. 13, Nov. 2022, doi: 10.1142/S0219887822502140.

[12] Y. Du and I. Mordatch, "Implicit Generation and Modeling with Energy Based Models," in Advances in Neural Information Processing Systems, 2019, vol. 32. [Online]. Available: https://proceedings.neurips.cc/paper_files/paper/2019/file/378a063b8fdb1db941e34f4bde584c7d-Paper.pdf

[13] Harder P, Watson-Parris D, Stier P, Strassel D, Gauger NR, Keuper J. Physics-informed learning of aerosol microphysics. Environmental Data Science. 2022;1:e20. doi:10.1017/eds.2022.22

[14] E. Guo, C. Zhou, S. Zhu, L. Bai, and J. Han, "Dynamic imaging through random perturbed fibers via physics-informed learning," Opt. Laser Technol., vol. 158, p. 108923, Feb. 2023, doi: 10.1016/j.optlastec.2022.108923.

[15] Kontoudis GP, Liarokapis M, Vamvoudakis KG and Furukawa T (2019) An Adaptive Actuation Mechanism for Anthropomorphic Robot Hands. Front. Robot. AI 6:47. doi: 10.3389/frobt.2019.00047

[16] Kim, U., Jung, D., Jeong, H. et al. Integrated linkage-driven dexterous anthropomorphic robotic hand. Nat Commun 12, 7177 (2021). https://doi.org/10.1038/s41467-021-27261-0

[17] Z. Zou, X. Meng, and G. E. Karniadakis, "Correcting model misspecification in physics-informed neural networks (PINNs)," Oct. 2023, [Online]. Available: http://arxiv.org/abs/2310.10776

[18] S. Moradi, N. Jaensson, R. Tóth, and M. Schoukens, "Physics-Informed Learning Using Hamiltonian Neural Networks with Output Error Noise Models," May 2023, [Online]. Available: http://arxiv.org/abs/2305.01338

[19] M. Raissi, P. Perdikaris, and G. E. Karniadakis, "Physics-informed neural networks: A deep learning framework for solving forward and inverse problems involving nonlinear partial differential equations," J. Comput. Phys., vol. 378, pp. 686–707, Feb. 2019, doi: 10.1016/j.jcp.2018.10.045.

[20] M. AlShabi and S. A. Gadsden, "Linear Estimation Strategies Applied to a Spring-Mass-Damper System," 2023 Advances in Science and Engineering Technology International Conferences (ASET), Dubai, United Arab Emirates, 2023, pp. 1-8, doi: 10.1109/ASET56582.2023.10180500.